POAC'17
Busan, KOREA

Proceedings of the 24th International Conference on
Port and Ocean Engineering under Arctic Conditions
June 11-16, 2017, Busan, Korea

Numerical Study on the Structural Response of Energy-Saving Device of Ice-Class Vessel due to Impact of Ice block

Sadaoki Matsui[1], Shotaro Uto[1], Yasuhira Yamada[1], Shinpei Watanabe[2]
[1] National Maritime Research Institute, Japan
[2] Nippon Kaiji Kyoukai, Japan

ABSTRACT

The present paper considers the contact between energy-saving device of ice-class vessel and ice block and clarifies the ice impact force and the structural response from various points of view. The contact analysis is performed by using LS-DYNA finite element code. The main collision scenario is based on Finnish-Swedish ice class rules and a stern duct model is used as an energy-saving device. For the contact force, two modelling approaches are adopted. One is dynamic indentation model of ice block based on the pressure-area curve. The other is numerical material modelling by LS-DYNA. The authors investigated the sensitivity of the structural response against the ice contact pressure, the interaction effect between structure and ice block, and the influence of eccentric collision. Furthermore, the simplified mechanical model was proposed to evaluate the structural response. The results of these simulations are presented and discussed with respect to structural safety.

KEY WORDS: Ice-class Vessel; Energy-saving Devise; Ice collision

INTRODUCTION

An energy-saving device is one of the most effective measures to improve propulsive efficiency in ice-free water. It is expected to be effective for ice-class vessels. However, its strength due to ice contact should be carefully considered in its design, and it is a significant technological issue to evaluate structural response due to impact of ice. Since some types of energy-saving devices are protuberant structure, they are strongly affected by dynamic factor such as oscillation. Therefore, "Time-domain" analysis is necessary instead of conventional "Static" estimation based on energy theory. Kinnunen et al (2013, 2015) implemented the contact analysis between ice and the azimuthing thruster. They indicated that the dynamic behavior of the structure affected the impact load significantly.

The purpose of the present study is to investigate the ice contact load and the structural response of the stern duct equipped for ice-class vessels. The main contact scenario is based on Finnish-Swedish ice class rules, and the used stern duct structure is Weather Adapted Duct (Kawasshima, et al. 2014) developed in National Maritime Research Institute, Japan. In this study, the authors carried out a series of non-linear dynamic finite element simulations to

evaluate the structural safety and estimate the ice contact load, including the effect of ice-structure interaction. For the ice contact load, two modelling approaches are adopted. One is dynamic indentation model of an ice block based on the pressure-area curve. The other is numerical material modelling by LS-DYNA to consider ice-structure interaction. For the evaluation of structural safety, the sensitivity analysis against the ice contact pressure was performed and thereby the simplified mechanical structural model was proposed. In addition to the structural response, the ice contact load was investigated in detail such as the effect of the structural interaction and the influence of eccentric collision.

ICE LOAD SCENARIOS

It is assumed that the ice block contacts to the front end of stern duct as shown in Figure 1. According to Finnish-Swedish Ice Class Rule (2010), the maximum design ice block entering the propeller is a rectangular ice block with the dimensions of $H_{\mathrm{ice}} \cdot 2H_{\mathrm{ice}} \cdot 3H_{\mathrm{ice}}$. The thickness of the ice block H_{ice} is given as 1.5[m] for ice-class 1A. The density of ice block ρ_{ice} was assumed to be 880[kg/m^3], and the added mass was given as the following equation. Only the added mass was considered as the fluid force effect.

$$M_{\mathrm{a}} = 1.82\rho H_{\mathrm{ice}}^3 \qquad (1)$$

The initial velocity of the ice block is assumed to be 5[knot] that is required as a vessel speed in the brash ice channels for the powering requirement of Finnish-Swedish ice class rules. These values are summarized in Table 1.

Table 1. Ice block basic parameter

Ice thickness H_{ice}	1.5[m]
Ice mass M_{ice}	17820[kg]
Ice added mass M_{a}	6296[kg]
Initial velocity v_0	2.572[m/s]

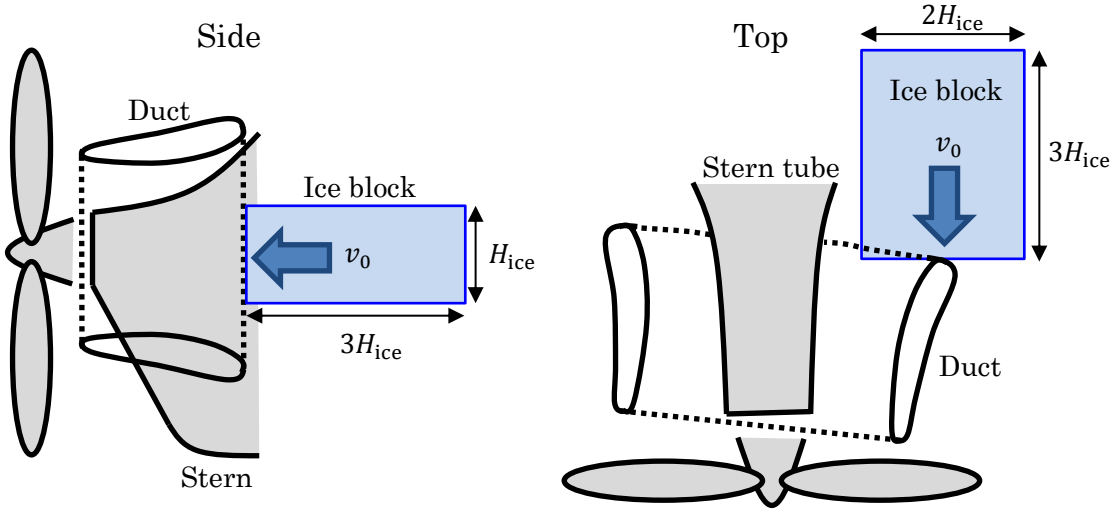

Figure 1. Contact between stern duct and ice block

ICE MODELLING

To perform safety evaluation, it is one of the most important processes to estimate an ice contact load. In this study, two load modelling approaches are adopted. One is the simple estimation model based on pressure-area curve (Daley, 1999). The ice load for structural requirement in UR-I (IACS, 2007) is based on this model. The other is FEM modelling. The dynamic contact simulation between ice block and structure was performed.

Load Model Based on Pressure-Area Curve

The general principles of the model are shown in Figure 2. The fore part of the stern duct is modelled to be rigid cylinder, and the indentation depth ζ_{n} can be obtained by the motion equation of an ice block.

$$(M_{\mathrm{ice}} + M_a)\ddot{\zeta_{\mathrm{n}}} = -F_{\mathrm{n}} \tag{2}$$

Here, the ice contact force F_{n} is expressed as a product of average contact pressure P and nominal contact area A:

$$F_{\mathrm{n}} = PA \tag{3}$$

Here, P is expressed as a function of A:

$$P(A) = P_0 A^{\mathrm{ex}} \tag{4}$$

Here, P_0 is average contact pressure at $A = 1[\mathrm{m}^2]$, and ex is an exponent constant. In this paper, the following equations are mainly used.

$$P(A) = 2.2A^{-1/3} \tag{5}$$

$$P(A) = 7.4A^{-0.7} \tag{6}$$

The equation (5) is proposed by Frederking and Ritch (2009) based on impact tests of bergy bit and ship. The equation (6) is proposed by Masterson (Palmer et al. 2009) for isolated small areas (<10 m^2), which is also recommended by the ISO code (ISO 19906, 2010). These relations are plotted with experimental data in Figure 3. The contact area is at most 0.5[m] in this simulation, hence the equation (6) gives much higher pressure. A is expressed as a function of indentation depth ζ_{n}:

$$A(\zeta_{\mathrm{n}}) = 2H\sqrt{2R\zeta_{\mathrm{n}} - \zeta_n^2} \tag{7}$$

by geometric consideration of indentation, regarding the fore part of the stern duct as a cylinder with a radius of R=0.13[m] as shown in Figure 2. Thus, F_{n} can be expressed by ζ_{n} and the load history $F(t)$ is obtained by solving the equation (2). To solve the differential equation, Runge-Kutta method was used. Both load curves based on equation (5) and (6) are called as "low" and "high" respectively and indicated in Figure 4. The termination of contact load is the moment when the indentation velocity is equal to zero. These areas are equal to the impulse of ice : $(M_{\mathrm{ice}} + M_{\mathrm{a}})v_0$.

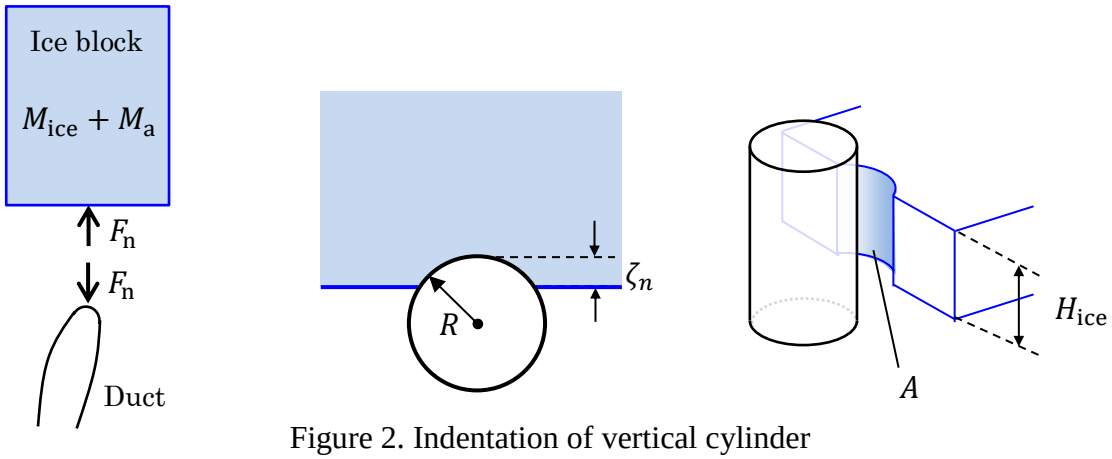

Figure 2. Indentation of vertical cylinder

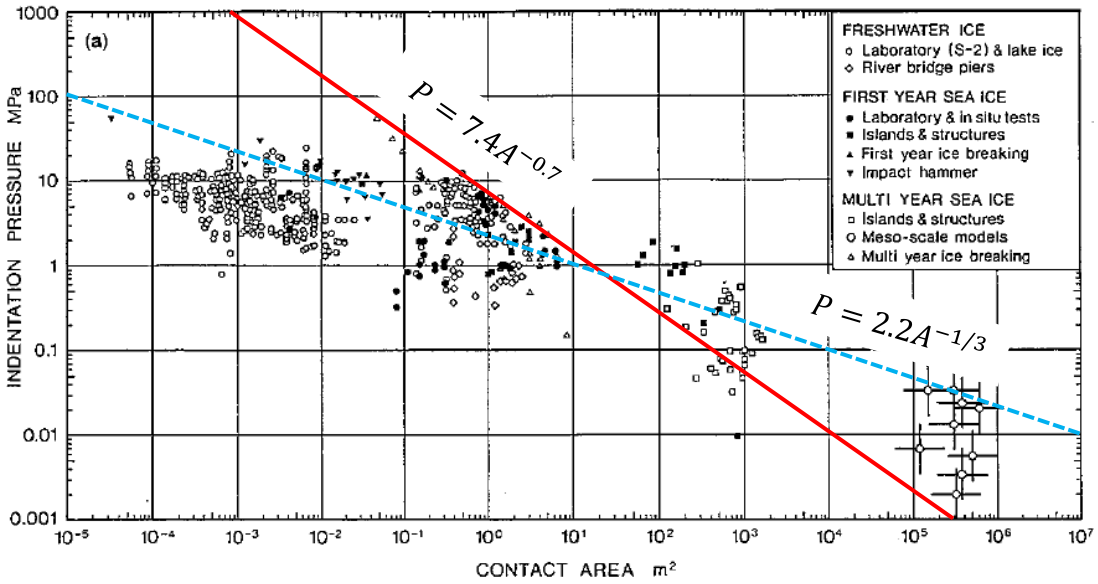

Figure 3. Pressure-area curve (Sanderson J.O.,1988)

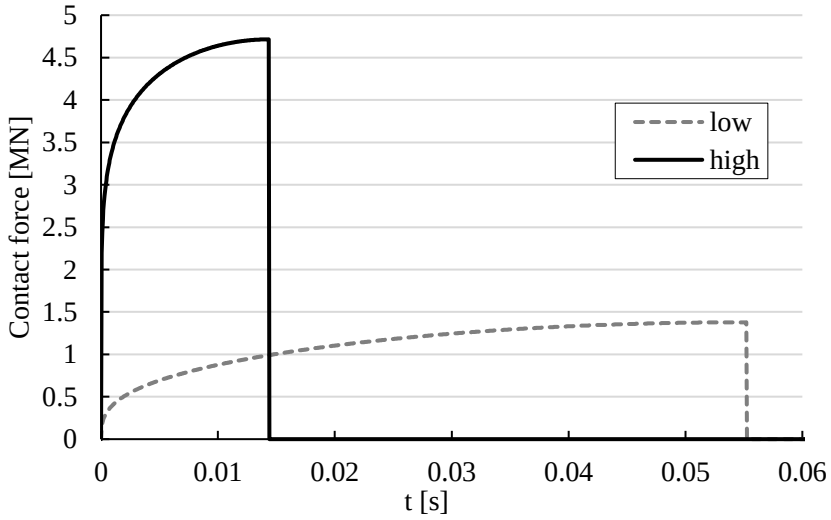

Figure 4. Time history of ice load

Finite Element Model

Several FEM modelling of ice have been tried and it was reported that they have a certain level of accuracy to estimate the contact force. The dynamic FEM analysis has been performed by using some material properties of ice calibrated already. To validate such theoretical models, the contact simulation between rectangular ice block and rigid cylinder with a radius of R=0.13[m] was performed. For the numerical simulation, LS-DYNA was chosen. The FEM models of the ice block and the cylinder are indicated in Figure 5. The ice material property was applied to only fine mesh zone and the remaining region was assumed to be a rigid body.

Gagnon (2011) calibrated volumetric strain-stress relationship based on MAT63 CRUSHABLE_FORM through the bergy bit field trial data. He carried out FEM simulation of the compression of the pyramid-shaped ice. He modelled several thin ice layers to express spalling behavior. The volumetric strain-stress relationships of the high and low pressure zone are expressed as shown in Figure 6. It should be noted that the high and low curves are considered separately although he combined them in his simulations. The young's modulus and Poisson's ratio is assumed to be 8[GPa] and 0.003, respectively.

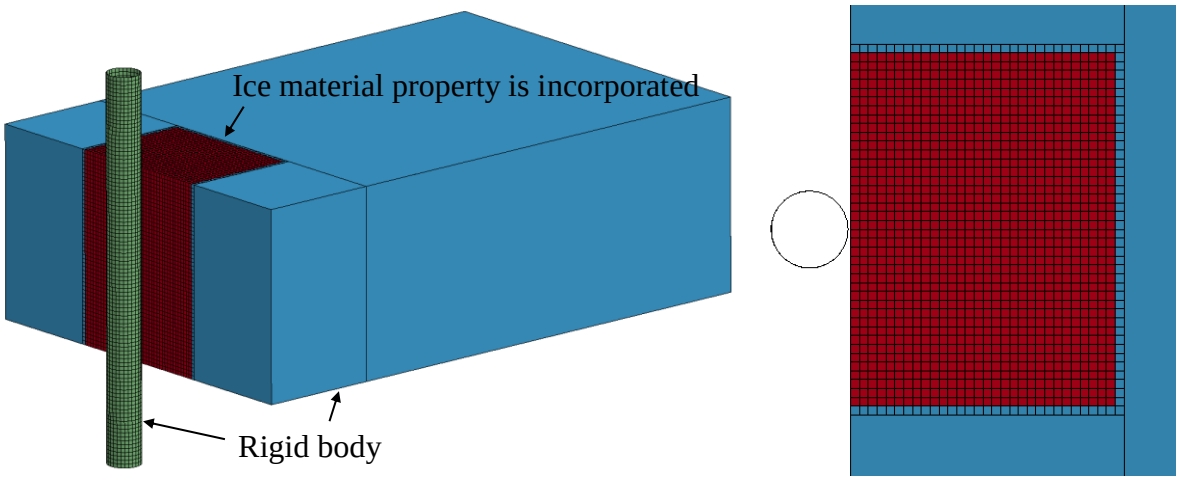

Figure 5. FEM model (Left: 3D view, Right: Top view)

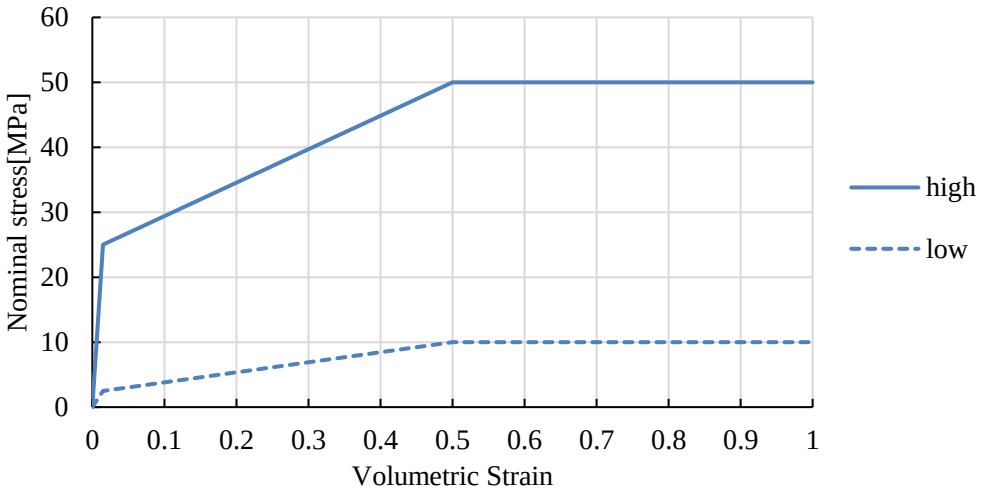

Figure 6. Relationship between nominal stress and volumetric strain

Liu (2011) used "Tsai-Wu" model as the yield criterion of ice:

$$f = J_2 - (a_0 + a_1 p + a_2 p^2) = 0 \tag{8}$$

where J_2 represents the second invariant of the deviatoric stress tensor s_{ij}, p is the hydrostatic pressure expressed in equation (9), and a_0, a_1 and a_2 are constants that require fitting to the triaxial experimental data. The equation (8) denotes the ellipsoid yield surface in the meridian plane. In this paper, the constant values of $a_0 = 22.93[\mathrm{MPa}^2]$, $a_1 = 2.06[\mathrm{MPa}]$, $a_2 = -0.023$ recommended by Derradji-Aouat (2000) are adopted.

$$J_2 = \frac{1}{2} s_{ij} s_{ji}, \quad p = -\frac{1}{3}\sigma_{ii} \tag{9}$$

Liu also defined failure criterion as follows.

$$\bar{\varepsilon}^p > \varepsilon_f \tag{10}$$

$$\bar{\varepsilon}^p = \sqrt{\frac{2}{3}\varepsilon_{ij}^p : \varepsilon_{ij}^p} \tag{11}$$

$$\varepsilon_f = \varepsilon_0 + \left(\frac{p}{p_2} - 0.5\right)^2 \tag{12}$$

where $\bar{\varepsilon}^p$ is the effective plastic strain, ε_f is the element failure strain, p_2 is the larger root of the yield function, ε_0 is the initial failure strain, which is assumed to be 0.01. Once the failure condition (10) is satisfied, the element fails and its stiffness is immediately set to zero in the numerical simulation. These material properties are defined in LS-DYNA using a MAT41_USE_DEFINED_MATERIAL_ MODELS which is defined by user subroutine. As a return mapping method for the yield surface, the cutting-plane algorithm (E. A. de Souza Neto, et. al, 2008) was used. The effect of strain rate and work hardening were not considered.

The time histories of the ice load are obtained by MAT 63 and MAT 41 and shown in Figure 7. In Figure 7, "MAT63 (high)" and "MAT63 (low)" correspond to the high and low stress model in Figure 6, respectively. For MAT 41, two cases that failure criterion of equation (10) is considered (Failure) or not (No Failure) are plotted. The two curves calculated by the pressure-area curve in Figure 4 are also indicated.

Two load curves of MAT 63 are consistent with the two load curves calculated by the pressure-area curve. On the other hand, "MAT41 (No Failure)" is consistent with the curve of high pressure model of pressure-area curve, whereas "MAT41 (Failure)" indicates the irrational intermittent behavior. This is because elements which satisfy the failure criterion are vanished immediately in the numerical calculation. In reality, crushed ice fragments also contribute to the compression stress in the contact area. Such the failure behavior strongly depends on the size of finite element and stress condition. The equation (10) is just pure empirical formula calibrated by Liu (2011), hence the failure criterion should be revised by the experiment in present condition. The indentation of the ice is treated by only continues behavior for such a reason, although the ice should behave in brittle failure mode in the present high strain rate condition. Further examination should be considered through an experiment in future.

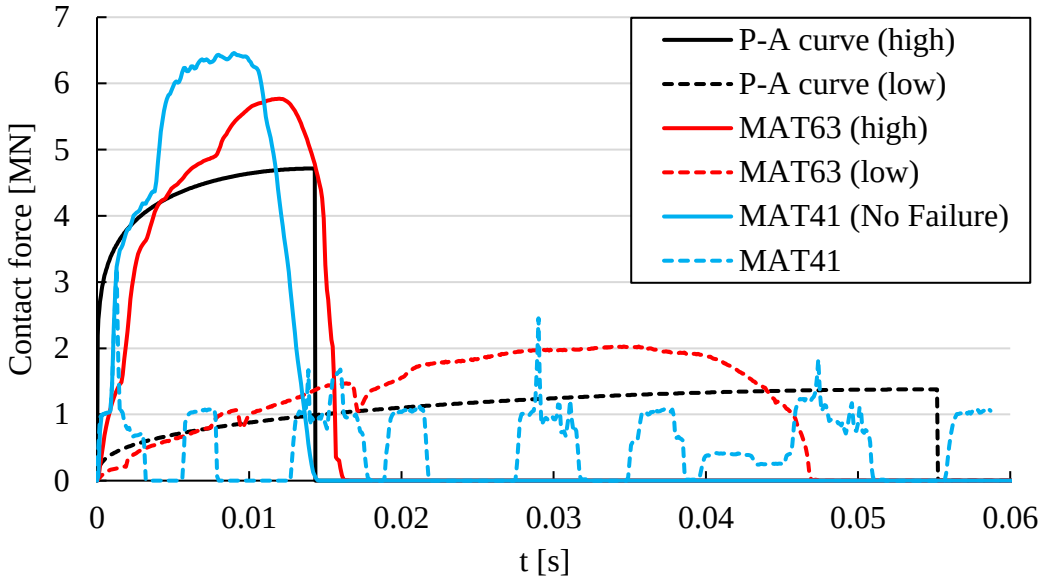

Figure 7. Time history of ice load

STRUCTURE MODEL

In this section, the FEM model of the stern and the duct structure and the calculation conditions are described. The detail of structural model and boundary conditions are described in Table 2, and the stern and the duct FEM model are shown in Figure 8. The junction between solid and shell element is modelled by Shell-Solid coupling model (Osawa, 2007).

Table 2. FEM analysis condition

Modelling region	Duct and stern model (35[m] from A.E.)
Element type	Bearing … solid element Another member … shell element
Thickness of duct	Inside web … 20[mm] Outside shell … 25[mm]
Material	Mild steel (MAT24) Young modulus … 206[GPa] Yielding stress … 235[MPa] Strain rate dependency … Cowper Symonds low
Boundary condition	Tight bulkhead of stern is fixed

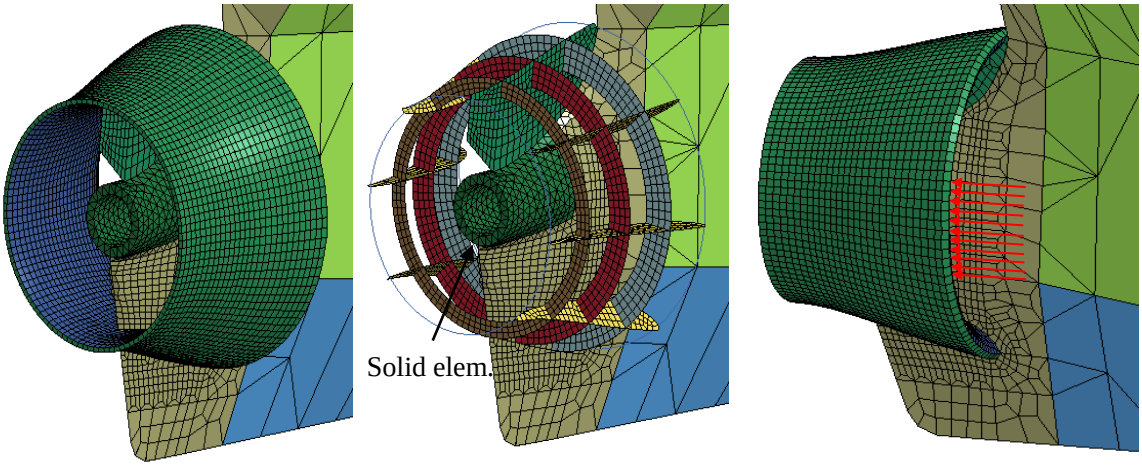

Figure 8. Structure FEM model

STRUCTURAL SENSITIVITY ANALYSIS

Since the contact pressure of ice has large uncertainty, the maximum contact load may have great variability even though the other conditions, such as mass and initial speed of the ice block, are the same. Accordingly, the structural sensitivity analysis against contact pressure is needed to evaluate the structural safety of the stern duct. Ice contact load based on the pressure-area curve are exerted at the fore part of the stern duct as nodal force as shown in the right figure of Figure 8. Those curves were calculated by equation (4), which ex is set to -1/3 and P_0 is changed, in the same manner as in Figure 4. Moreover, those were modified to sinusoidal curves while keeping each maximum force and area (impulse) the same. This is because of avoiding the irrational oscillation in the structure due to the step of load curve at the end of indentation, which is generated by the absence of ice elasticity. An actual load curve might take the medium form of the both curves. Some examples of used load curves are shown in Figure 9.

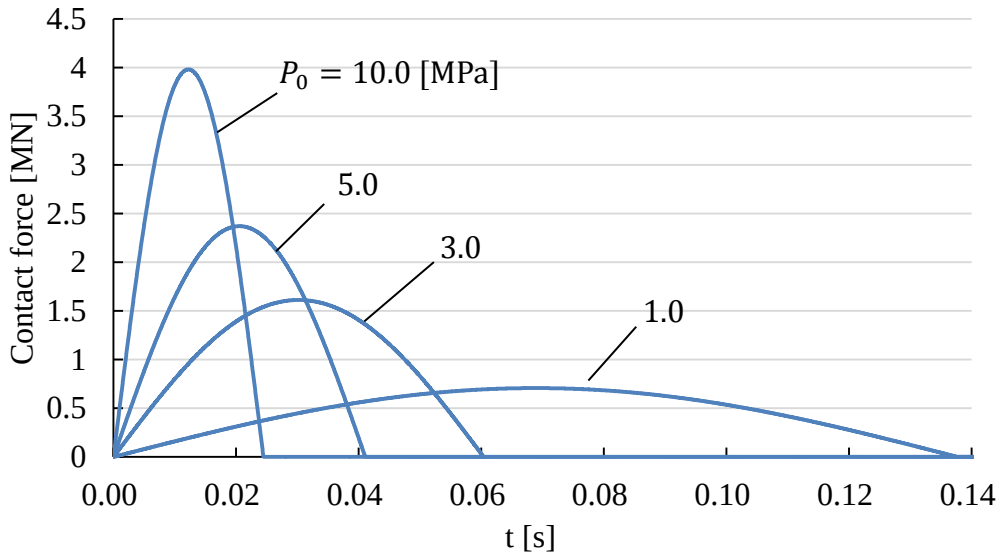

Figure 9. Load curves under changing contact pressure (ex $= -1/3$)

Figure 10 shows an example of Von-Mises stress distribution on the stern duct at the moment when the maximum stress occurs. As the general response of the stern duct, it was found that the relatively high stress occurs in connection of duct and hull, X and Y in Figure 10. The sensitivity of the maximum Von-Mises stress value at X and Y are shown in Figure 11. The broken line indicates the tolerance stress value in CSR-B (IACS, 2006) and is 280[MPa] when the element size is less than 200[mm]. Figure 11 indicates that the larger response occurs as the nominal pressure increases even though the impulses of curves are the same value. This is because that the maximum force becomes large as P_0 becomes large and the acting time approaches to the quarter of the eigenperiod of the stern duct, which is about 0.05[s]. In the case that the acting time is enough long, the external force does negative work while the stern duct turns back by elastic behavior. It is also found in Figure 11 that the maximums stress occurs at X when P_0 is smaller than 4.5[MPa] and stress at Y is larger beyond this value. This is because the static horizontal bending is dominant when P_0 is small and the position of X is affected by this effect mainly. Meanwhile, the dynamic effects such as free oscillation are remarkable when P_0 is large and the extremely large tensile stress is induced at Y which is the connection between duct and hull.

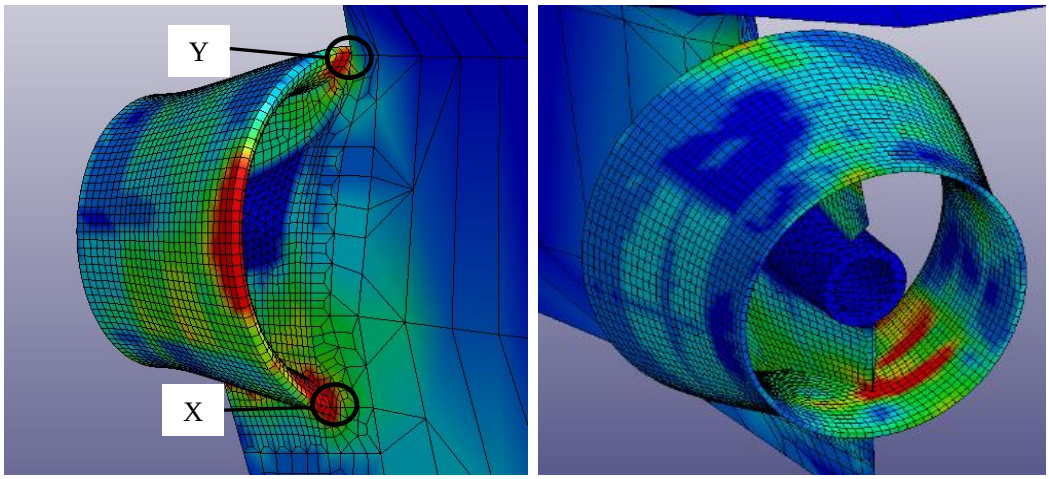

Figure 10. Von-Mises stress distribution (Red : High ↔ Blue : Low)

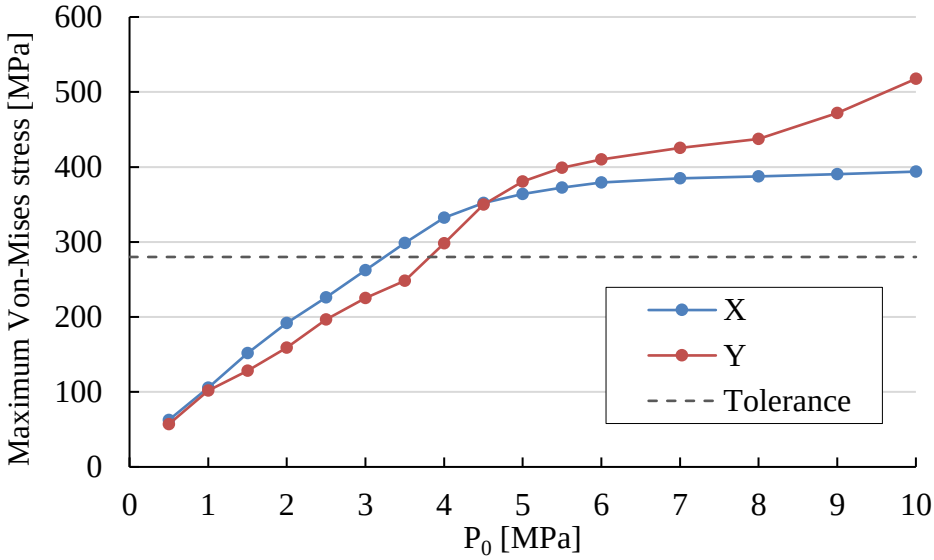

Figure 11. Sensitivity of the maximum Von-Mises stress on the stern duct against nominal contact pressure

The maximum displacement of the point where load acts in aft direction is shown in Figure 12. In addition to the result by LS-DYNA, the result by proposed simplified model "MCK model" is also indicated. MCK model means single-degree-of-freedom spring-dumper-mass model:

$$M\ddot{\xi} + C\dot{\xi} + K\xi = F_{\mathrm{n}} \tag{13}$$

Here, ξ is the displacement of the stern duct at the contact point in aft direction, M, C, K are mass, damping and spring coefficient of the stern duct, respectively. These responses correspond reasonably, although the stern duct is significantly complex structure which consists of duct, stern tube, and other local members. This is because the maximum displacement occurs in the first amplitude of oscillation, and the value is determined by the most dominant component of oscillations. For this reason, the MCK model can express the maximum response of the structure accurately.

For the simplification into MCK model, it is necessary to determine the constant of mass, damper and spring coefficients. These values should be estimated by moment of inertia, structural damping, and horizontal bending stiffness of the stern duct respectively. In this paper, these constants are calibrated by results of LS-DYNA. If the relationship between the displacement and the local stress becomes clear, the structural response of the stern duct would be able to estimate by using MCK model.

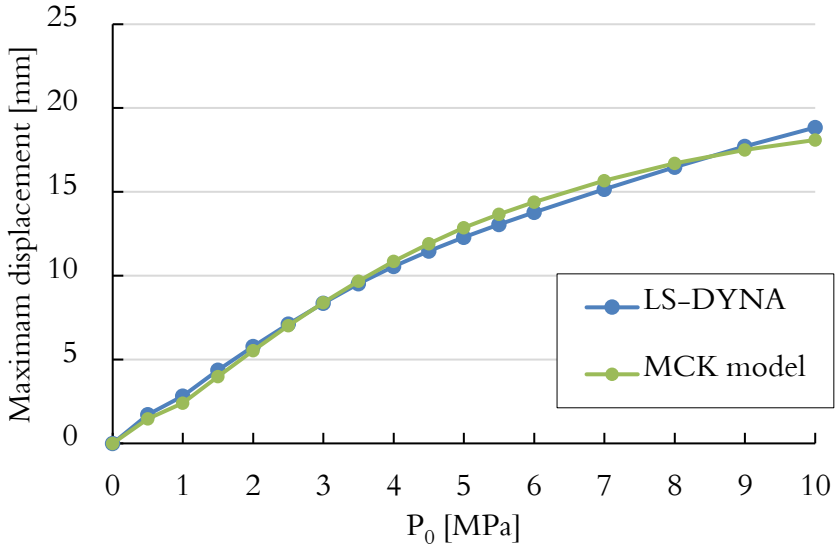

Figure 12. Maximum displacement of the point where load acts

EFFECT OF SHIP-ICE INTERACTION ON THE ICE LOAD

To obtain the ice contact load, steel structures can be assumed to be a rigid body in general because there is a large difference of rigidity between the ice and the steel structure. Meanwhile, in case of the protuberant structure such as a stern duct, oscillation occurs significantly by an impact force and the structural response may affect the impact load. To investigate such influence quantitatively, the simulation were performed with a stern duct of rigid (hereafter called as decouple) and compliant body (couple) and both contact loads were compared. The used FEM model is shown in Figure 13. MAT63 (high) and MAT63 (low) were applied to only fine mesh zone and the remaining region was assumed to be rigid body.

The contact point and the center of gravity of the ice block are in the straight line in the direction of contact velocity to avoid rotation of the ice. Each load history is shown in Figure 14. The reason why the peak load of the decouple simulations are smaller than the results of MAT 63 in Figure 7 is that the collision angle must be applied because of the stern shape, and the contact area is smaller than the case that regards the stern duct as a cylinder.

Figure 14 shows that the contact force by the couple analysis is smaller than that by the decouple analysis in high-stress model but the little difference is seen in low-stress model. The difference of both tendencies can be explained by the deformation of the stern duct. The history of displacement of the stern duct at the contact position and the center of gravity of the ice block in collision direction by the couple analysis is shown in Figure 15. The contact load is primarily determined by the indentation depth, e.g. the difference of the displacements between the stern duct and the ice block. Consequently, the contact load is reduced by the displacement of the stern duct in the couple analysis. The influence of the displacement of the stern duct is relatively large in the case of high-stress model, on the other hand, that is relatively small in the case of low-stress model. From these facts, it is presumed that the ice-structure interaction effect becomes greater as the contact pressure is higher. However, if the acting time is much less than the eigenperiod of the structure, the structural displacement hardly occurs and the interaction effect may become small conversely. In the present analysis, the influence of the structural response was at most 20% and it is smaller than the uncertainty of ice property.

ECCENTRIC CONTACT ANALYSIS

In the actual collision, the contact position and the center of gravity of ice are not always in line. Thus the initial kinematic energy is absorbed partly into the rotational energy of the ice block by eccentric collision and the contact load should be somewhat reduced. To clarify the reduction of the contact load against the eccentricity, the eccentric contact analysis was performed by LS-DYNA. The material property of ice is assumed to be MAT63 (high), and the structure is assumed to be a rigid body. The six cases in different eccentricities, 0, 0.3, 0.6, 0.9 1.2, 1.45[m] (The half breadh of ice block is 1.5[m]) were performed. The contact load histoiry is shown in Figure 16. Reduction of the contact load by eccentricity can be seen clearly. Since no marked differences are found in the shape of these curves, the magnitude of the load may be estimated by only its impulse. The impulse due to collision can be derived from momentum theory, and the following relations are derived in the case that the slip at the contact point is allowed or not :

$$P_{\text{slip}} = \frac{I}{I + e_y^2 m} m v_0 \tag{14}$$

$$P_{\text{non-slip}} = \frac{I + e_x^2 m}{I + \left(e_x^2 + e_y^2\right) m} m v_0 \tag{15}$$

where m, I, v_0 are the mass, the moment of inertia and the initial velocity of the ice block, respectively, e_y is the eccentric distance, and e_x is the distance between the contact position and the center of gravity of the ice block in the collision direction. The completely plastic collision is assumed because the plastic behavior is dominant in the ice property. The derivation of the above formulae are described in APPENDIX in detail. The influence of the eccentricity against the impulse is shown in Figure 17. Ecah value is normalized by the value

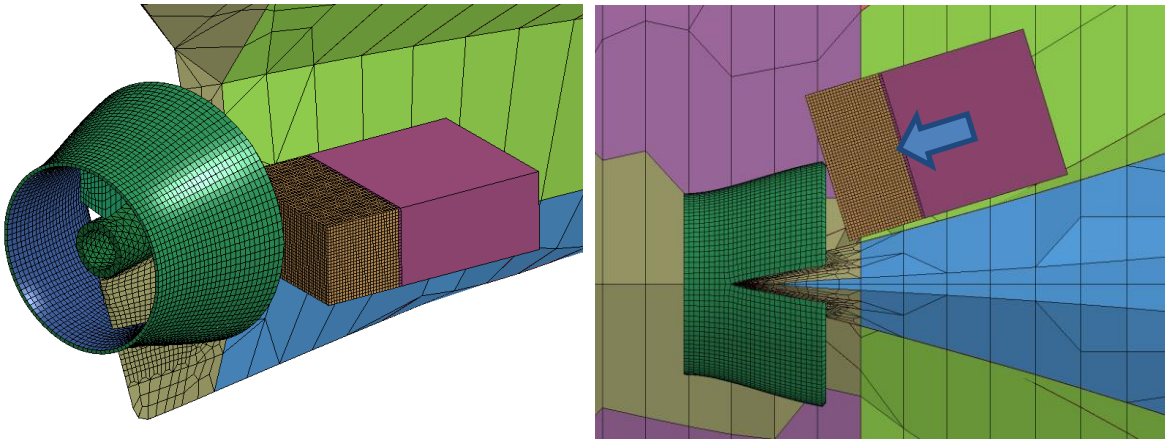

Figure 13. FEM model of stern duct and ice block (Left: 3D view, Right: Bottom view)

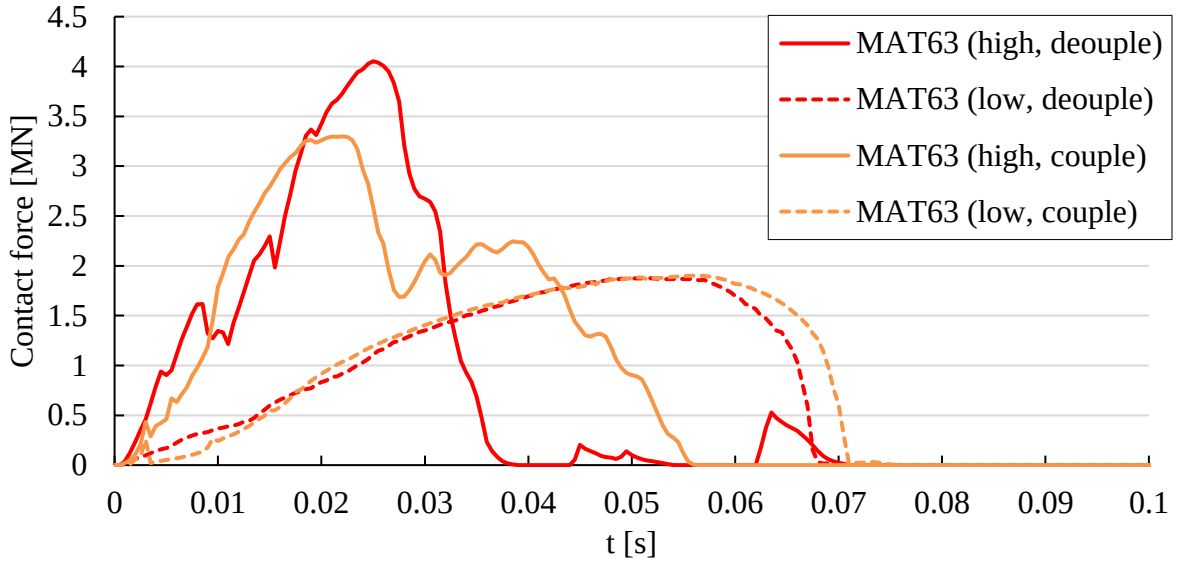

Figure 14. Load history of couple and decouple analysis

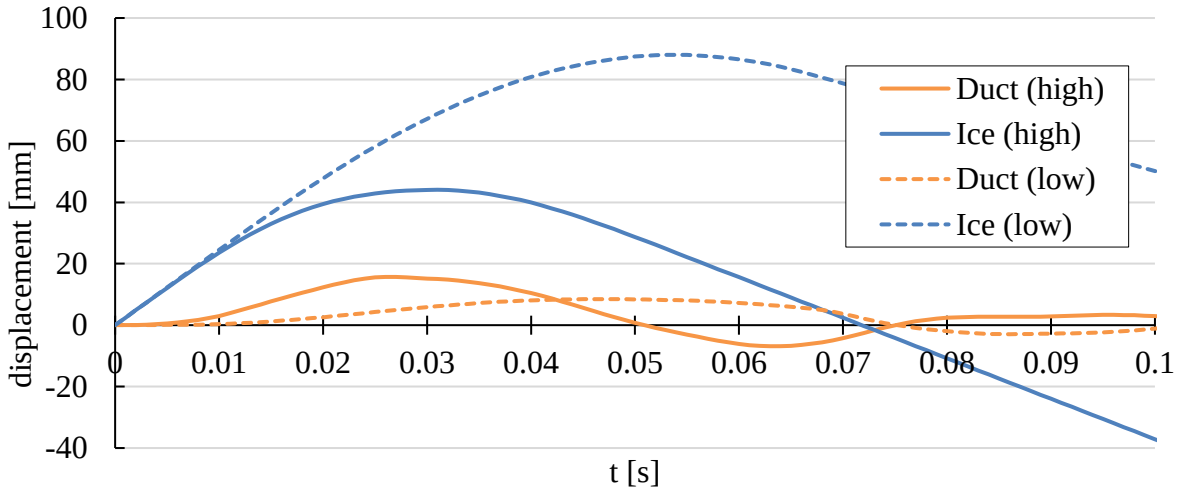

Figure 15. Displacement history of the stern duct and the ice block

of non-eccentric collision. In addition to the results of LS-DYNA, the equation (14) and (15) are also indicated. The results of LS-DYNA almost correspond with the momentum theory of the non-slip case, and these reductions are small in comparison with the momentum theory of the slip-allowed case. This is because the ice block is indented into the edge of the stern duct and the center of rotation corresponds to the contact position, and thus the rotational motion of the ice block is hard to occur in comparison with the slip-allowed case. On the other hand, for example, the ice contact with hull does not cause indentation, hence its tendency may be close to slip-allowed case.

It is indicated from the result that the load reduction by the eccentric collision is not so large against the structure such as the stern duct, and to simulate under non-eccentric collision scenario does not result in overestimation for the structural safety. Such tendency becomes remarkable when the distance between the contact position and the center of gravity of the ice block e_x is large.

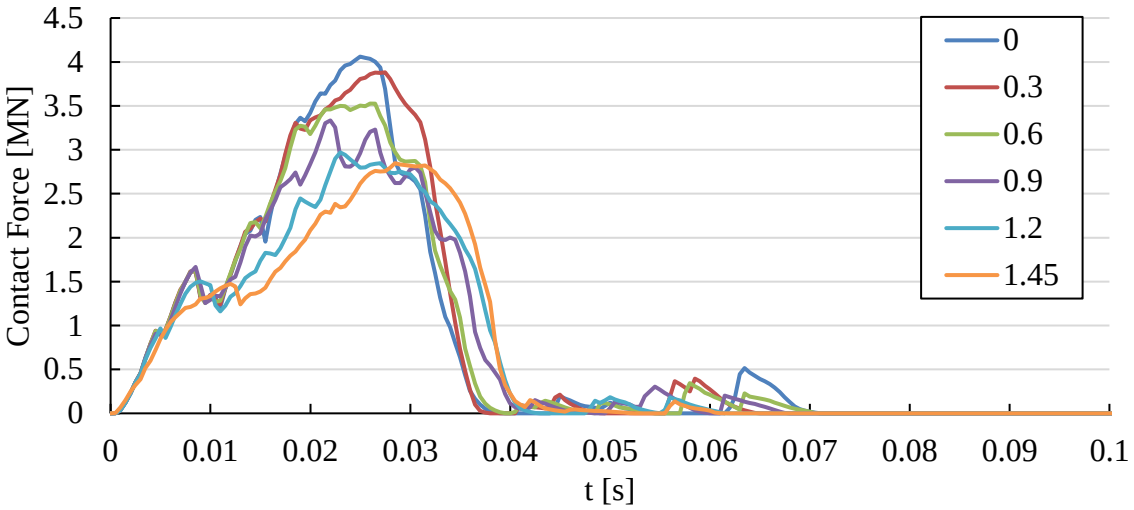

Figure 16. Time history of eccentric contact load

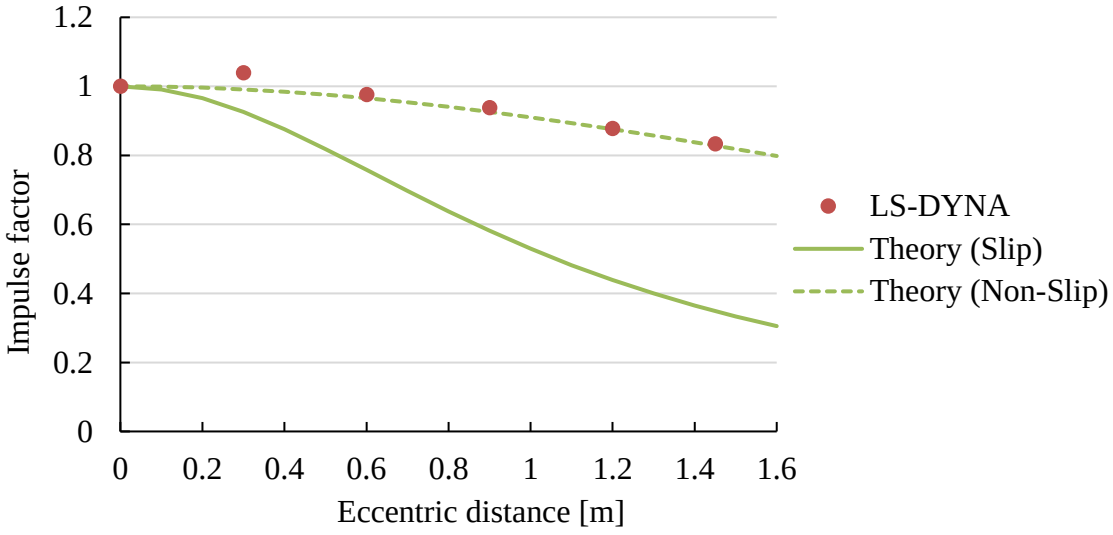

Figure 17. Eccentric effect on contact force

CONCLUSIONS

The evaluation of structural safety of the stern duct due to the impact of ice block was performed through the series of dynamic FEM analysis. Several conclusions are described as follows.

About the structural response:

- The structural response becomes large as contact pressure of ice becomes high even though the impulses are the same.
- Relatively high stress occurs in the connection of the duct and the hull. There is a possibility that the maximum stress in the structure exceeds the permissible stress depending on the contact pressure.
- The maximum deformation of the stern duct due to impact force can be expressed by the single-degree-of-freedom spring-damper-mass model accurately. This model may apply the simple estimation for occurring stress in the structure.

About the contact load:

- The ice contact load reduces by considering the ice-structure interaction. The reduction is large as the contact pressure becomes high, but the influence of the interaction was at most 20% in the present case and is smaller than the uncertainty of ice property.
- The reduction of ice contact load due to the eccentric effect is relatively small because the contact point becomes the center of rotation of the ice block because of indentation. Accordingly, the safety evaluation based on non-eccentric collision analysis is not over-estimation for thin column structure such as the present structure.

In this study, the incorporated material model of ice in FEM analysis was validated indirectly comparing with the theoretical model based on the pressure-area curve. However, only the yield criterion is defined as continuous behavior, and it can't express the tendency of real ice that the contact pressure becomes large as the contact area becomes small due to the non-simultaneity of contact between ice and structure. This tendency can be imitated to some extent by introducing the failure criterion properly, as mentioned by Liu (2011) and Gao (2015). In order to carry out such modelling, the examination of the criteria and the mesh size in detail should be performed and verified by experiments.

ACKNOWLEDGEMENTS

This research was carried out jointly by Oshima Shipbuilding Co., Ltd., and ClassNK as part of the ClassNK Joint R&D for Industry Program.

REFERENCES

Aki Kinnunen, Pekka Koskinen, Maria Tikanmaki, 2015. ICE-STRUCTURE IMPACT CONTACT LOAD CALCULATION WITH DYNAMIC MODEL AND SIMPLIFIED LOAD FORMULA, *Port and Ocean Engineering under Arctic Conditions,* June 14-18 2015, Trondheim, Norway

Aki Kinnunen, Maria Tikanmaki, Jaakko Heinonen, Juha Kurkela, Pekka Koskinen, Matti Jussila, 2013. Azimuthing thrusters ice impact load calculation, *Azimuthing thrusters ice class rule development Steering group meeting*, 2013-10-31

Claude Daley: ENERGY BASED ICE COLLISION FORCES, Expanded version (full derivations) of paper for POAC 99, Proc. of the 15th International Conference on Port and Ocean Engineering under Arctic Conditions, Helsinki University of Technology in Espoo, Finland on August 23-27, 1999.

Derradji-Aouat, A., 2000. A unified failure envelope for isotropic fresh water ice and iceberg ice, *Offshore mechanics and arctic engineering : presented at ETCE/OMAE 2000 Joint Conference*, Vol. 2, Part B, pp. 1241-1248.

E.A. de Souza Neto, D. Peric, D. R. J. Owen, 2008. Computational Method for Plasticity : Theory and Applications

Frederking, R. & Ritch, R. 2009. The nature of the process pressure-area relation from CCGS Terry Fox bergy bit impacts. 19th (2009) International Offshore and Polar Engineering Conference, June 21, 2009 – June 26, 2009. Osaka, Japan: *International Society of Offshore and Polar Engineers*. pp. 608-613. ISSN 10986189

Gagnon, R.E., 2011. A numerical model of ice crushing using a foam analogue, *Cold Region Science and Technology*, Vol. 65, pp.335-350.

H. Kawashima, K. Kume, N. Sakamoto, 2014. Study of Weather Adapted Duct, *Reports of National Maritime Research Institute, 2014*, Vol. 14-2, pp. 19-34.

ISO/CD 19906, 2010. Petroleum and Natural Gas Industries-Arctic Offshore Structures, ISO TC 67/SC 7/WG 8, *Final Draft International Standard. International Standardization Organization*, Geneva, Switzerland p. 434.

IACS, 2007, Requirements concerning POLAR CLASS, Unified requirements

IACS, 2006, COMMON STRUCTURAL RULES FOR BULK CARRIERS

IMO, 2012. DEVELOPMENT OF MANDATORY CODE FOR SHIPS OPERATING IN POLAR WATERS, *SUB-COMMITTEE ON SHIP DESIGN AND EQUIPMENT*, 57th session Agenda item 11,

Liu, Z., et al., 2011. Plasticity based material modelling of ice and its application to ship-iceberg impacts, *Cold Regions Science and Technology*, Vol. 65, pp. 326-334.

N. Osawa, K. Hashimoto, J. Sawamura, T. Nakai, S. Suzuki, 2007. Study on shell-solid coupling FE analysis for fatigue assessment of ship structure, *Marine Structures*, Vol. 20, pp. 143-163.

Palmer, A. C., Dempsey, J.P. & Masterson, D. M. 2009. A revised ice pressure-area curve and a fracture mechanics explanation. *Cold Regions Science and Technology*, Vol. 56, pp. 73-76.

Sanderson J.O., Ice Mechanics, Risks to Offshore Structures

TRAFI, 2010. *ICE CLASS REGULATIONS 2010 "FINNISH-SWEDISH ICE CLASS RULES 2010"*, TRAFI/31298/03.04.01.00/2010

Yan Gao, Zhiqiang Hu, et al, 2015. An elastic-plastic ice material model for ship-iceberg collision simulations, *Ocean Engineering*, Vol. 102, pp. 27-39

APPENDIX

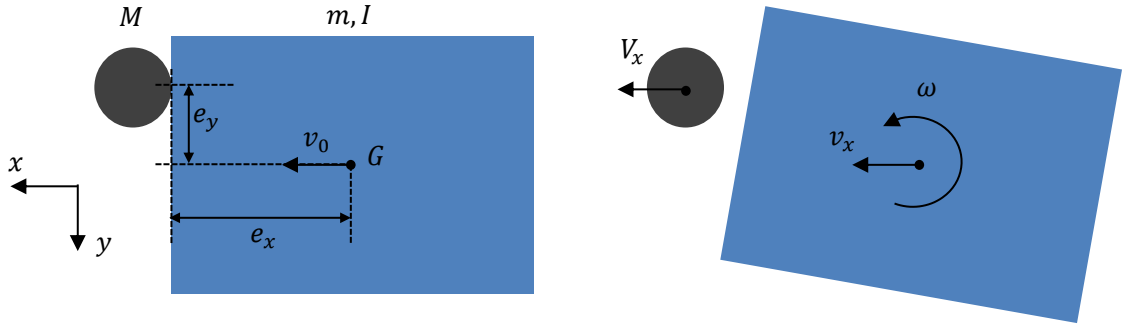

Let us assume that an ice block which has mass m and moment of inertia I collides against a point mass in an initial velocity v_0 and an eccentiricity e_y, and after collision, the velocity of the point mass V_x and the ice block v_x and angular velocity of the ice block ω are generated. The difinition of the direction is shown in the above figure.

In the case of completely plastic collision, the relative velocity in x direction between the ice block and the point mass after collision is equal to zero. Consequently, V_x, v_x, ω can be obtained by the law of conservation of momentum and angular momentum and the equation of the relative velocity after collision.

$$\begin{cases} mv_0 = MV_x + mv_x \\ 0 = Me_yV_x + I\omega \\ V_x = v_x + e_y\omega \end{cases} \tag{16}$$

Accordingly, V_x, v_x, ω can be written as follows.

$$\begin{cases} V_x = \dfrac{m}{1+m+\mathcal{I}}v_0 \\ v_x = \dfrac{1}{1+m}\left(m + \dfrac{\mathcal{I}}{1+m+\mathcal{I}}\right)v_0 \\ \omega = -\dfrac{\mathcal{I}}{1+m+\mathcal{I}}\dfrac{v_0}{e_y} \end{cases} \tag{17}$$

where

$$m = \frac{m}{M}, \quad \mathcal{I} = \frac{e_y^2 m}{I}$$

The impulse of collision is described as follows.

$$P_{\text{slip}} = M(V_x - 0) = \left(\frac{1}{1+m+\mathcal{I}}\right)mv_0 \tag{18}$$

If M is infinity, the impulse approaches to the following value.

$$P_{\text{slip}} = \frac{I}{I + e_y^2 m}mv_0 \tag{19}$$

In the case of completely plastic collision and non-slip condition at the contact point, center of the rotation of the ice block corresponds to the contact point. If the mass is infinite, the law of conservation of angular momentum can be described:

$$-e_y m v_0 = \{I + (e_x^2 + e_y^2)m\}\omega \tag{20}$$

and v_x is written as:

$$v_x = -\omega e_y = \frac{e_y^2 m}{I + (e_x^2 + e_y^2)m} v_0 \tag{21}$$

Finally, the impulse of collision in non-slip condition is obtained as follows.

$$P_{\text{non-slip}} = -m(v_x - v_0) = \frac{I + e_x^2 m}{I + (e_x^2 + e_y^2)m} m v_0 \tag{22}$$